Electronic Supplementary Material (ESI) for Physical Chemistry Chemical Physics.

Electronic Supplementary Information of Fermi Resonance in Solvated H_3O^+: A Joint Experimental and Theoretical Study on Ar-tagged and Ne-tagged H_3O^+

Qian-Rui Huang†, Tomoki Nishigori§, Marusu Katada§, Asuka Fujii§*, and Jer-Lai Kuo†*

† Institute of Atomic and Molecular Sciences, Academia Sinica, Taipei 10617, Taiwan

§ Department of Chemistry, Graduate School of Science, Tohoku University, Sendai 980-8578, Japan

*E-mail: jlkuo@pub.iams.sinica.edu.tw (J. –L. K.); asukafujii@m.tohoku.ac.jp (A.F.)

Contents:

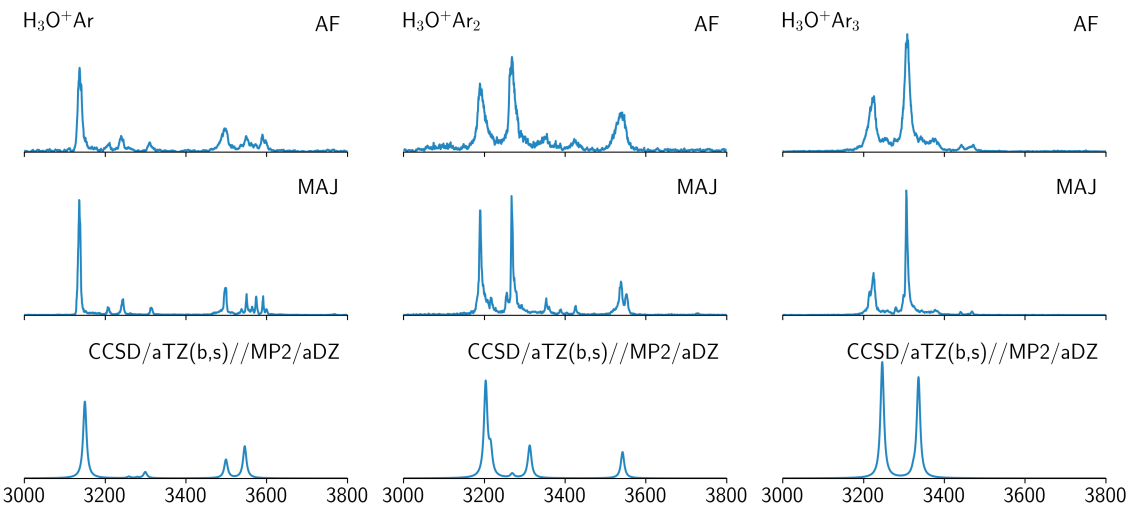

Figure S1 Comparison on the measured IR spectra of H_3O^+…Ar_n (n=1, 2, and 3) in this work and the spectra measured by Mark A. Johnson's group. [1,2] The two sets of spectra are essentially same.

Contamination of the spectrum of H_3O^+…Ne_1

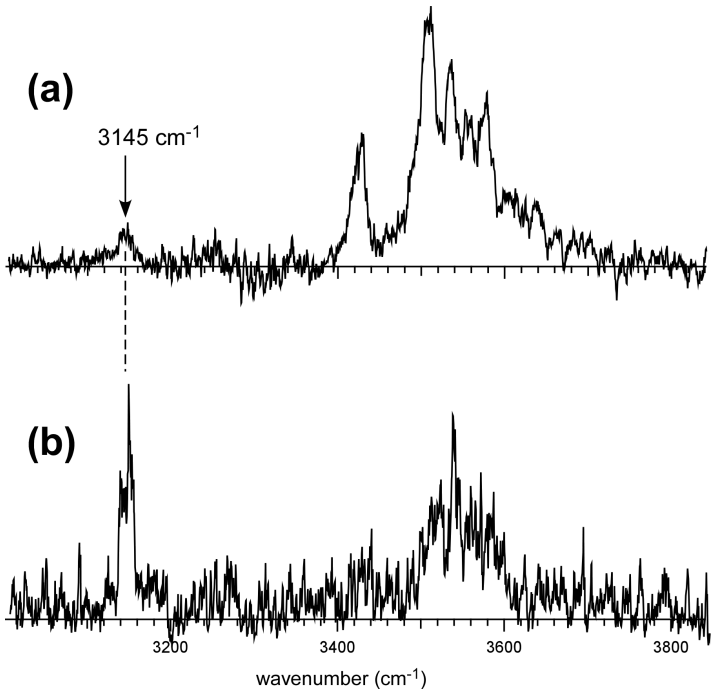

Figure S2 IR spectra of H_3O^+…Ne_1 (m/z = 39) by monitoring (a) m/z = 19 (H_3O^+) and (b) m/z = 18 fragment channels. Note that spectrum (b) is not averaged enough to have the equal quality of spectrum (a). At 3145 cm^{-1}, an intense band appears in spectrum (b), and its band position is same as the weak band indicated by the arrow in spectrum (a). The band intensity patterns of these two spectra are very different each other. Therefore, the weak band at 3145 cm^{-1} in spectrum (a) cannot be attributed to H_3O^+**…**Ne_1, but it should come from the spectral contamination due to the lack of the mass resolution in the second mass spectrometer. The spectral carrier of the 3145 cm^{-1} band is not identified at present.

The importance of individual terms in nMR

In many systems, the most important part of the potential surface can be described with few-body components; hence, the different terms in Eq. 1 has different contributions to the whole system, and we can enhance the efficiency significant without losing much accuracy by including only these important terms. Furthermore, to improve accuracy, we can calculate important part of potential energy surface with high-level methods.

We assume that the terms with larger magnitudes have greater importance in describing the total interaction. For each term in Eq. 1, the magnitude of the term can be calculated as taking an average of the absolute term value over all grid points. Figure S2 shows the relative magnitude of all terms in H_3O^+…RG_n (RG=Ne and Ar and n=1, 2 and 3). In all cases, terms corresponding to only stretching modes have a larger magnitude, which should have higher importance; on the contrary, bending modes only show moderate amplitude on 1-body terms, and all other terms (including 2-body cross terms) show small magnitude. Therefore, we decide to replace the terms relevant to (1) 2 bending modes and (2) 3 stretching modes with results from higher level calculations. (1) is a bit more than expected, but the additional computational effort is acceptable since the number of needed grid points is not very many for one 2-body term.

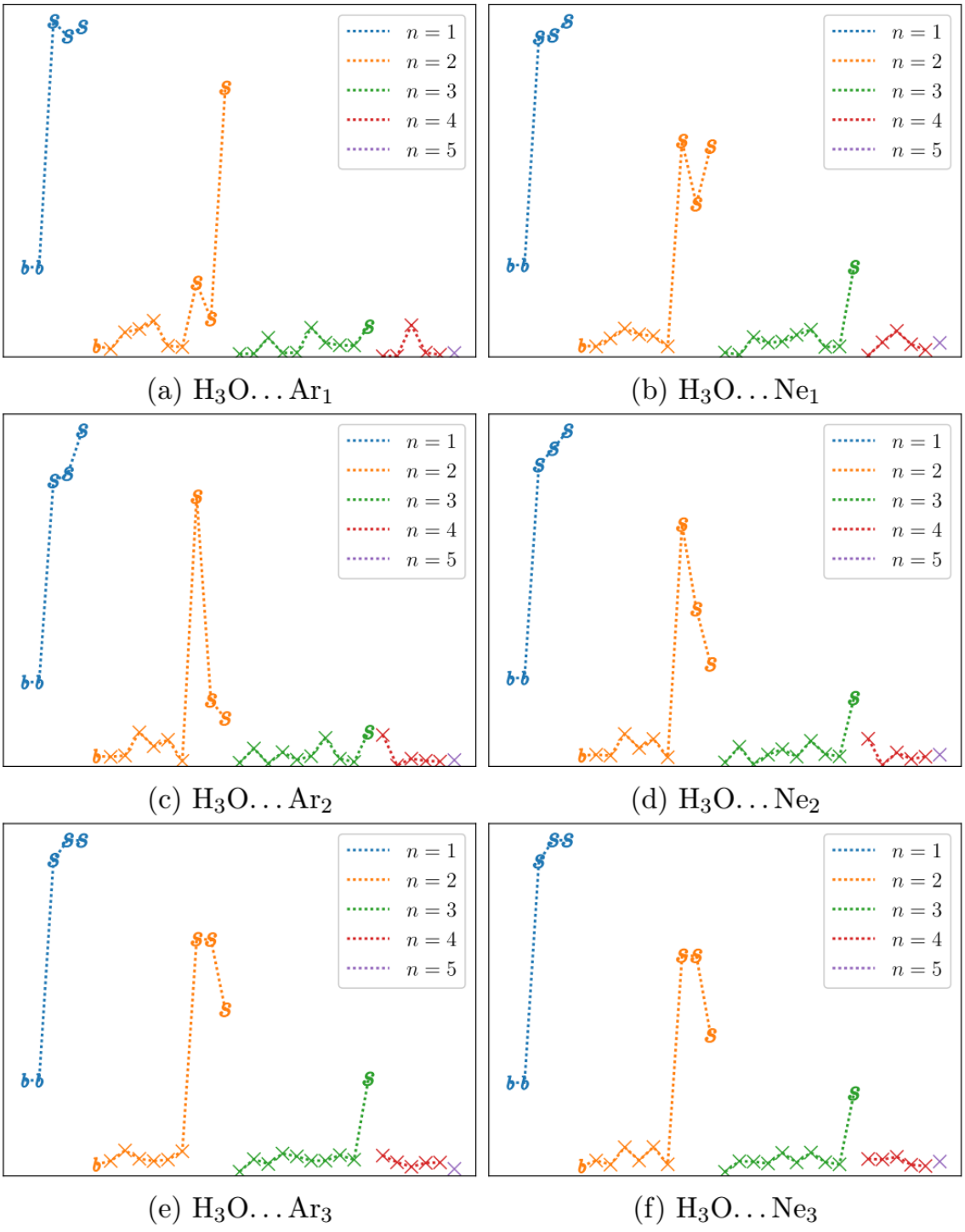

Figure S3 The relative magnitude of all $\Delta V_{\{i\}}^{(n)}$ terms in H_3O^+…RG_n (RG=Ne and Ar and n=1, 2, and 3). The terms corresponding to **only bending modes** and **only stretching modes** are denoted by **b** and **s**, respectively; all other terms corresponding to normal modes from both bending and stretching modes are denoted by crosses. Terms with different n are plotted with different colors.

Table S1. Cartesian coordinates of H_3O^+…RG_n (RG=Ne & Ar, n=1, 2, and 3) optimized by MP2/aug-cc-pVDZ.

H_3O^+…Ne_1

O	0.041478	-1.389739	-0.000000
H	-0.007909	-0.405174	-0.000000
H	-0.369351	-1.765892	0.809110
H	-0.369351	-1.765892	-0.809110
Ne	0.041478	1.505487	0.000000

H_3O^+…Ne_2

O	0.025558	1.020740	-0.000000
H	-0.678818	1.704353	-0.000000
H	-0.018409	0.467310	0.813430
H	-0.018409	0.467310	-0.813430
Ne	0.025558	-0.540245	2.448311
Ne	0.025558	-0.540245	-2.448311

H_3O^+…Ne_3

O	0.000000	0.000000	0.553467
H	0.000000	0.937626	0.255173
H	-0.812008	-0.468813	0.255173
H	0.812008	-0.468813	0.255173
Ne	0.000000	2.818995	-0.173108
Ne	-2.441321	-1.409498	-0.173108
Ne	2.441321	-1.409498	-0.173108

H_3O^+…Ar_1

O	-0.030111	1.932293	-0.000000
H	0.003472	0.937498	-0.000000
H	0.389702	2.300782	0.807049
H	0.389702	2.300782	-0.807049
Ar	-0.030111	-1.166523	0.000000

H_3O^+…Ar_2

O	0.016812	1.337934	-0.000000
H	-0.712256	1.993187	-0.000000
H	-0.013735	0.778172	0.818343
H	-0.013735	0.778172	-0.818343
Ar	0.016812	-0.395917	2.603747
Ar	0.016812	-0.395917	-2.603747

H_3O^+…Ar_3

O	0.000000	0.000000	0.744212
H	0.000000	0.940387	0.436810
H	-0.814399	-0.470194	0.436810
H	0.814399	-0.470194	0.436810
Ar	0.000000	3.027277	-0.134521
Ar	-2.621698	-1.513638	-0.134521
Ar	2.621698	-1.513638	-0.134521

Table S2: Matrix elements ($\langle b', s' | \mathbb{H} | b, s \rangle$) for the six quantum states involved in Fermi Resonance of all $H_3O^+ \ldots RG_n$ (RG=Ne & Ar, n=1, 2, and 3) calculated at MP2/aTZ//MP2/aDZ and CCSD/aDZ//MP2/aDZ level.

$H_3O^+ \ldots Ar_1$ MP2/aTZ//MP2/aDZ

3189.2	-1.2	0.0	13.1	37.9	0.0	
-1.2	3203.0	0.0	-28.6	23.9	0.0	
0.0	0.0	3202.9	0.0	0.0	43.2	
13.1	-28.6	0.0	3034.5	7.8	0.0	31.4
37.9	23.9	0.0	7.8	3396.0	0.0	44.8
0.0	0.0	43.2	0.0	0.0	3457.7	43.2

$H_3O^+ \ldots Ar_1$ CCSD/aDZ//MP2/aDZ

3208.7	0.0	-1.7	9.8	38.8	0.0	
0.0	3218.4	0.0	0.0	0.0	41.5	
-1.7	0.0	3218.2	30.7	-18.1	0.0	
9.8	0.0	30.7	3092.1	7.7	0.0	32.2
38.8	0.0	-18.1	7.7	3399.4	0.0	42.8
0.0	41.5	0.0	0.0	0.0	3460.5	41.5

$H_3O^+ \ldots Ar_2$ MP2/aTZ//MP2aDZ

3188.7	0.0	1.7	-21.7	0.0	-30.5	
0.0	3201.3	0.0	0.0	-37.1	0.0	
1.7	0.0	3206.0	-22.0	0.0	31.8	
-21.7	0.0	-22.0	3109.3	0.0	6.6	30.9
0.0	-37.1	0.0	0.0	3107.0	0.0	37.1
-30.5	0.0	31.8	6.6	0.0	3448.4	44.1

$H_3O^+ \ldots Ar_2$ CCSD/aDZ//MP2/aDZ

3206.2	0.0	0.8	-20.6	0.0	31.0	
0.0	3215.1	0.0	0.0	37.6	0.0	
0.8	0.0	3219.0	23.6	0.0	28.5	
-20.6	0.0	23.6	3159.2	0.0	-6.3	31.4
0.0	37.6	0.0	0.0	3162.3	0.0	37.6
31.0	0.0	28.5	-6.3	0.0	3451.0	42.1

$H_3O^+ \ldots Ar_3$ MP2/aTZ//MP2/aDZ

3192.2	0.0	-0.2	31.6	-0.9	-0.4	
0.0	3203.9	0.0	0.1	17.7	-33.3	
-0.2	0.0	3205.5	-0.8	-33.3	-17.8	
31.6	0.1	-0.8	3157.6	0.0	0.1	31.6
-0.9	17.7	-33.3	0.0	3171.7	0.0	37.7
-0.4	-33.3	-17.8	0.1	0.0	3172.0	37.7

$H_3O^+ \ldots Ar_3$ CCSD/aDZ//MP2/aDZ

3207.6	0.0	0.2	-32.0	-1.1	0.5	
0.0	3216.3	0.0	-0.1	17.7	33.4	
0.2	0.0	3218.0	-1.0	33.4	-17.7	
-32.0	-0.1	-1.0	3203.6	0.0	0.1	32.0
-1.1	17.7	33.4	0.0	3221.8	0.0	37.8
0.5	33.4	-17.7	0.1	0.0	3222.0	37.8

$H_3O^+ \ldots Ne_1$ MP2/aTZ//MP2/aDZ

3199.1	0.0	-0.4	30.6	29.0	0.0	
0.0	3212.9	0.0	0.0	0.0	-43.4	
-0.4	0.0	3215.0	-27.6	33.1	0.0	
30.6	0.0	-27.6	3306.7	6.1	0.0	41.2
29.0	0.0	33.1	6.1	3397.6	0.0	44.0
0.0	-43.4	0.0	0.0	0.0	3442.1	43.4

$H_3O^+ \ldots Ne_1$ CCSD/aDZ//MP2/aDZ

3218.5	0.0	-0.3	29.7	27.4	0.0	
0.0	3229.0	0.0	0.0	0.0	-41.9	
-0.3	0.0	3231.4	26.3	-32.6	0.0	
29.7	0.0	26.3	3323.0	5.1	0.0	39.7
27.4	0.0	-32.6	5.1	3405.6	0.0	42.6
0.0	-41.9	0.0	0.0	0.0	3446.1	41.9

$H_3O^+ \ldots Ne_2$ MP2/aTZ//MP2/aDZ

3205.6	0.0	0.7	35.5	0.0	21.4	
0.0	3218.7	0.0	0.0	-43.6	-0.1	
0.7	0.0	3221.8	19.9	0.0	-37.7	
35.5	0.0	19.9	3309.2	0.0	4.0	40.6
0.0	-43.6	0.0	0.0	3355.6	0.0	43.6
21.4	-0.1	-37.7	4.0	0.0	3434.4	43.4

$H_3O^+ \ldots Ne_2$ CCSD/aDZ//MP2/aDZ

3224.6	0.0	0.0	33.7	0.0	-21.1	
0.0	3234.5	0.0	0.0	42.6	0.0	
0.0	0.0	3237.7	20.0	0.0	36.1	
33.7	0.0	20.0	3324.3	0.0	-3.4	39.2
0.0	42.6	0.0	0.0	3376.8	0.0	42.6
-21.1	0.0	36.1	-3.4	0.0	3439.4	41.8

$H_3O^+ \ldots Ne_3$ MP2/aTZ//MP2/aDZ

3212.5	-0.2	0.1	-40.3	-0.3	0.3	
-0.2	3224.6	0.0	0.1	-39.7	-16.9	
0.1	0.0	3226.1	-0.4	16.9	-39.8	
-40.3	0.1	-0.4	3314.8	0.0	0.0	40.3
-0.3	-39.7	16.9	0.0	3372.2	0.0	43.2
0.3	-16.9	-39.8	0.0	0.0	3372.3	43.2

$H_3O^+ \ldots Ne_3$ CCSD/aDZ//MP2/aDZ

3231.7	0.2	0.1	38.9	-0.1	0.4	
0.2	3240.7	0.0	-0.1	38.8	16.5	
0.1	0.0	3242.4	0.4	16.5	-38.8	
38.9	-0.1	0.4	3329.4	0.0	0.0	38.9
-0.1	38.8	16.5	0.0	3391.4	0.0	42.1
0.4	16.5	-38.8	0.0	0.0	3391.5	42.2

References

1 S. G.Olesen, T. L.Gausco, G. H.Weddle, S.Hammerum and M. A.Johnson, *Mol. Phys.*, 2010, **108**, 1191–1197.

2 A. B.McCoy, T. L.Guasco, C. M.Leavitt, S. G.Olesen and M. A.Johnson, *Phys. Chem. Chem. Phys.*, 2012, **14**, 7205–7214.